Atomic-scale Analysis of Solute Segregation Energy into Grain Boundaries and Polycrystals

ATOMIC-SCALE ANALYSIS OF SOLUTE SEGREGATION ENERGY INTO GRAIN BOUNDARIES AND POLYCRYSTALS

A Thesis Presented

by

Tara Nenninger

to

The Faculty of the Graduate College

of

The University of Vermont

In Partial Fulfillment of the Requirements
for the Degree of Master of Science
Specializing in Mechanical Engineering

January, 2022

Defense Date: November 12, 2021
Thesis Examination Committee:

Frederic Sansoz, Ph.D., Advisor
Laura Webb, Ph.D., Chairperson
Jihong Ma, Ph.D.
Cynthia J. Forehand, Ph.D., Dean of the Graduate College

ABSTRACT

Solute segregation in grain boundaries (GBs) is used in design to stabilize nanocrystalline alloys. While analyzing GB segregation energy as a spectrum allows for a more in-depth analysis of the effects of GB atomic structure on solute segregation, this method inherently ignores solute-solute interaction by nature of considering one solute at a time. Here we develop an efficient molecular statics (MS) algorithm for determining the local effect of solute-solute interaction on GB segregation. We apply this algorithm to a Σ9 (221) symmetric tilt grain boundary in a bicrystal as well as a randomly oriented polycrystal for Ni and Cu solutes in Ag. The findings suggest that small changes in average segregation energy between one and two solutes correlate directly to the effect of a fixed solute on its local environment through solute-solute interactions. This work shows that this methodology succeeds to accelerate the study of complex segregation behavior such as heterogeneous and homogeneous tendencies.

ACKNOWLEDGEMENTS

I would like to thank my advisor Dr. Frederic Sansoz and my committee members Dr. Laura Webb and Dr. Jihong Ma for their support and insights throughout this process. I would also like to express my gratitude for the past and present members of my cohort as well as my friends and family for their encouragement.

This research was supported by the U.S. Department of Energy grant number DE-SC0020054 as well as computational resources from the National Energy Research Scientific Computing Center (NERSC), a U.S. Department of Energy Office of Science User Facility located at Lawrence Berkeley National Laboratory, operated under Contract No. DE-AC02-05CH1123. This research was also supported by computational resources from the Extreme Science and Engineering Discovery Environment (XSEDE), which is supported by National Science Foundation grant number ACI-1548562.

TABLE OF CONTENTS

Page

LIST OF TABLES

LIST OF FIGURES

CHAPTER 1: Introduction

1.1. Background

1.1.1. Nanocrystalline Materials

Materials scientists have been highly interested in nanocrystalline (NC) materials for more than three decades [1] largely due to their unique properties compared to metals of the same composition with larger grain sizes. NC metals are defined as metals with an ordered lattice structure and a grain size less than 100 nm. NC metals have been shown to have increased strength, hardness, and favorable fatigue behavior due to dislocation motion resistance, all of which have been accredited to the increased grain boundary (GB) volume fraction [2-4]. However, NC materials are thermodynamically unstable and exhibit grain growth or coarsening because GB atoms have higher intrinsic energy than atoms in the bulk of the grain. Due to GB atom disorder, atoms diffuse from GBs to the bulk of the grain to lower the total energy of the material by increasing the grain size [5]. This is undesirable because the mechanical properties that make NC materials interesting are dependent on their small grain size, e.g. Hall-Petch grain-size strengthening effects [3].

To maintain NC stability and avoid coarsening, a preferred method of structural stabilization is alloying with a solute that segregates to the GBs [4, 6]. GB segregation occurs when solute atoms are in a lower energy state in the grain boundary than in the bulk of the material. This stabilizes the NC structure by ensuring that grain growth and solute migration will not lead to a further relaxed state. Solute segregation can stabilize GBs thermodynamically, by lowering the GB energy, or kinetically, by pinning GB migration with solute clusters or precipitates. The characteristic parameter used to determine whether a solute-lattice alloy will segregate is called GB segregation energy. Accurately calculating the GB segregation energy and understanding segregation behavior of a solute-lattice pair is key for NC alloy design.

1.1.2. Segregation Energy

An early model of equilibrium solute segregation at GBs was made by McLean in 1957 [7]. This model relates the actual fraction of solute in the GB, X_b, the GB fraction available for solute, X_b^0, the free energy per mole of solute, ΔG, and the bulk solute, X_c, given as:

$$\frac{X_b}{X_b^0 - X_b} = \frac{X_c}{1 - X_c} \exp\left(\frac{-\Delta G}{RT}\right), \tag{1}$$

where ΔG is estimated by finding the difference in elastic strain energy of a bulk atom versus a solute atom,

$$E_{el} = \frac{24\pi K \mu_0 r_0 (r_1 - r_0)^2}{3K + 4\mu_0}, \tag{2}$$

where K is the bulk modulus of the solute, r_0 is the atomic radius of the matrix atoms, r_1 is the radius of the solute atoms, and μ_0 is the matrix shear modulus. The free energy per mole of solute can be related to GB segregation energy as:

$$\Delta G = \Delta E_{seg} + T\Delta H \tag{3}$$

Since segregation energy calculations are treated as molecular statics, T here is 0 K, thus the segregation energy can be considered equal to the free energy, leading to modern usages of Equation 1 in the form:

$$\frac{X_{gb}}{1 - X_{gb}} = \frac{X_c}{1 - X_c} \exp\left(\frac{\Delta E_{seg}}{kT}\right), \tag{4}$$

where X_{gb} is the same as X_b defined above, and k is Boltzman's constant. Here, the equation for ΔE_{seg} is the difference in energy of a solute atom in the GB and in the bulk,

$$\Delta \mathrm{E}_{\mathrm{seg}} = \mathrm{E}_{\mathrm{solute}}^{\mathrm{gb}} - \mathrm{E}_{\mathrm{solute}}^{\mathrm{c}} \tag{5}$$

This model relies on the assumption that all GBs are one entity, thus there is one representative ΔE_{seg}. Recent atomistic simulation studies have shown that GB segregation energy can be more accurately described by a spectrum of energies for each GB atomic site, which follows a skew-normal distribution [8-10]. The following equations have been developed to capture this spectrality based on atom site types:

$$X^{tot} = (1 - f^{gb})X^c + f^{gb} \sum_i F_i^{gb} \left[1 + \frac{1-X^c}{X^c} \exp\left(\frac{\Delta E_i^{seg}}{kT}\right)\right]^{-1}, \tag{6}$$

where X^{tot} is the global solute concentration, f^{gb} is the fraction of atomic sites that are in the GBs, and F_i^{gb} is the atomic site fraction of each site type *i* in the GB. This equation accounts for the fractional distribution of GB solute atoms across GB sites and how their energies form an average grain boundary segregation energy that is fit to the skew normal distribution of the E_{seg} spectrum [9]. This new model can be related to Equation 4 with an effective average segregation energy:

$$\Delta \overline{\mathrm{E}_{\mathrm{seg}}^{\mathrm{eff}}} = \frac{1}{\overline{\mathrm{X}^{\mathrm{gb}}}\left(1 - \overline{\mathrm{X}^{\mathrm{gb}}}\right)} \sum_{\mathrm{i}} \mathrm{F}_{\mathrm{i}}^{\mathrm{gb}} \, \Delta \mathrm{E}_{\mathrm{i}}^{\mathrm{seg}} \mathrm{X}_{\mathrm{i}}^{\mathrm{gb}} \left(1 - \mathrm{X}_{\mathrm{i}}^{\mathrm{gb}}\right) \tag{7}$$

This model is more accurate than the McLean model as it captures the distribution across different GB sites. It was also noted that solute-solute interaction did not influence the distribution of solute atoms in GB sites, and thus solutes follow a homogeneous distribution at GBs [9]. However, by nature of testing each GB atom site one at a time with only one solute atom, the effect of solute-solute interactions cannot be determined using this method. It is perhaps more accurate to say that in random GBs, there is no distinctly heterogeneous pattern in the probability that a solute will segregate to a specific GB site. However, there are documented examples of heterogeneous segregation behavior [11-13], so while this model captures a more accurate representation of segregation behavior than the McLean model, it cannot be used to fully describe the segregation behavior of all solute-lattice material combinations.

1.1.3. Homogeneous vs. Heterogeneous Segregation

Solute segregation behavior has been shown to occur in two ways: homogeneously and heterogeneously. Until recently, all GB segregation was assumed to be homogeneous, with the solute atoms evenly distributed across all GBs with no distinct clustering behavior. However, there have been notable examples of distinctly heterogeneous segregation behavior in two different bulk-solute alloys— specifically Pt-Au and Ag-Ni [11, 13-16].

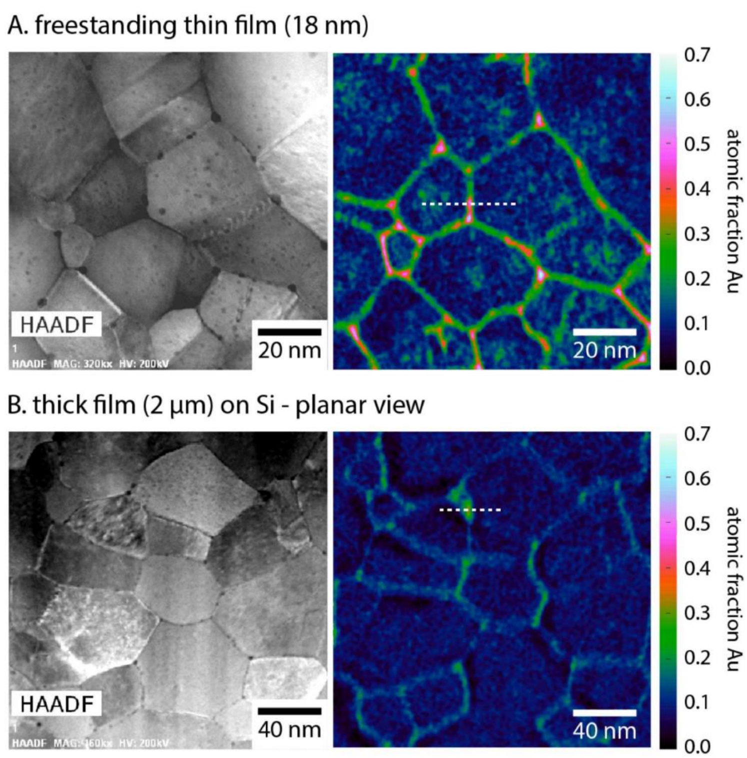

Figure 1: Heterogeneous Au segregation in Pt films [13].

The first model was FCC Pt alloyed with small amounts of Au. Two-phase segregation behavior was found experimentally in both thick and thin films of $Pt_{90}Au_{10}$ [13]. Specifically, the local atomic percentage of Au in the GBs showed distinct high concentrations of solute segregation among the mean segregation behavior. Theoretical Monte-Carlo/Molecular Dynamics (MC/MD) simulations of multiple ordered grain boundaries on Pt bicrystals with the same Au concentration showed phase separation within the grain boundary, implying that heterogeneous segregation behavior would occur in ordered GBs as well as the random GBs in the experimental polycrystalline films. Further study of this alloy produced different experimental heterogeneous GB segregation using multiple annealing temperatures and showed that this mode of GB segregation inhibited grain growth significantly [14].

The other example is FCC Ag alloyed with small amounts of Ni. This study showed two distinct heterogeneous behaviors on low and high energy ordered GB bicrystals [11]. Preferential GB selection as well as clustering within the GB were both observed, implying that multiple types of heterogeneity can exist within grain boundaries as well as the solute clustering in GB junctions observed in Pt-Au. It was also shown that solute concentration level affected the heterogeneous segregation behavior but not the homogeneous segregation in both the high and low energy ordered GB bicrystals. Since heterogeneous and homogeneous behavior were found in the same Ag lattice, solute-solute interactions with a preference for dipole formation are seen to be an indicator for heterogeneous segregation [11]. Further simulation of heterogeneous Ni segregation showed suppression of shear localization in polycrystalline Ag where homogeneous Cu segregation did not [15].

Since heterogeneous segregation behavior is a relatively new field of study, it is unclear how different segregation behavior affects the material properties of the alloy. However, it is safe to say that it will be important to distinguish homogeneous or heterogeneous behavior when choosing a bulk-solute pair for commercial application.

1.2. Motivation

GB segregation in NC alloys has been shown to produce significantly stronger and more stable materials. However, while previous research has generated a relatively comprehensive database of alloy combinations to determine propensity for segregation, the one solute segregation energy spectra do not allow for any further analysis on segregation behavior in the presence of solute-solute interactions. While solute concentration affects segregation behavior, clustering must start from nucleation. Creating a simple algorithm that could add this layer of analysis without significantly increasing computational requirements will aid in NC materials design.

1.3. Hypothesis

Solute segregation in a polycrystal that is characterized as either homogeneous or heterogeneous relates to the distribution of atomic segregation energies in the presence of solute-solute interactions.

1.4. Thesis Objectives

The primary objective of this thesis is to study the effects of solute-solute interaction on segregation energy spectra in bicrystals and polycrystals by developing a simple MS algorithm with a particular focus on Ag-Cu and Ag-Ni alloys where Cu and Ni solute elements are predicted to segregate homogeneously and heterogeneously, respectively, in Ag GBs.

1.5. Thesis Organization

Chapter 2 presents the methodology. Segregation energy results for the bicrystal and polycrystal are presented and discussed in Chapter 3 and Chapter 4, respectively. Chapter 5 draws the major conclusions and some suggestions for further research.

CHAPTER 2: Methodology

MS simulations were performed using the Large-scale Atomic/Molecular Massively Parallel Simulator (LAMMPS) [17], run across two bulk-solute material pairs. The first was Ag-Ni, which used an embedded-atom method Finnis-Sinclair potential developed by Pan et al. [11]. This potential was specifically developed for the simulation of Ni solutes in Ag grain boundaries. This cross potential fit existing Ag and Ni potential data to ab initio calculations on liquid $Ag_{80}Ni_{20}$ and included Ni dipole formation energy to account for Ag-Ni and Ni-Ni interactions in single crystals and grain boundaries. The second was Ag-Cu, which used the Wu et al. EAM alloy potential [18]. This potential was fit and optimized for surface diffusivity using density functional theory calculations of Cu on Ag. This potential was shown to be suitable for other heteroepitaxial systems, such as GBs [19, 20].

2.1 Molecular Statics Algorithm

For each model (bicrystal and polycrystal), a list of GB atoms was generated from the visualization software OVITO [21] by calculating the centrosymmetry parameter with a minimum threshold of 0.01. An atom from this list was iteratively selected as a solute, i.e. all atoms in the generated atomistic model were set to Ag type, except for one GB atom designated by the GB list which was set to the solute type. The model was then energy minimized at 0 K using conjugate gradient method, with energy (eV) and force (eV/Å) tolerance stopping criteria of 10^{-8} and maximum evaluations set to 10^{3} evaluations. The final minimized energy of the total system was exported to a separate data file along with the particle identifier of the solute atom for that evaluation. In the following iteration, all atom displacements were deleted, and the GB atom selected was moved to the next entry in the GB list. Each iteration was completed by jumping back to the loop marker until the last GB atom variable entry was evaluated. Reinitializing the model on each iteration ensured that the minimal energy configuration for each solute atom was not influenced by the previous configuration.

2.2 Atomistic Models

2.2.1. Bicrystal

The simulated bicrystal was a Σ9 (221) symmetric tilt GB with a periodic simulation box of dimensions 5.3 nm x 10 nm x 3.5 nm, which correlates to six coincident site lattices in the x-direction. The model contained two grains with two grain boundaries in the x-z plane. Figure 2(a) shows the lattice vectors for the grains in the x, y, and z directions, respectively. The upper grain was initially shifted by (2, 0, 1) Å to obtain the standard E structural units that characterize the Σ9 (221) GB structure in the literature as shown in Figure 2(b) [22].

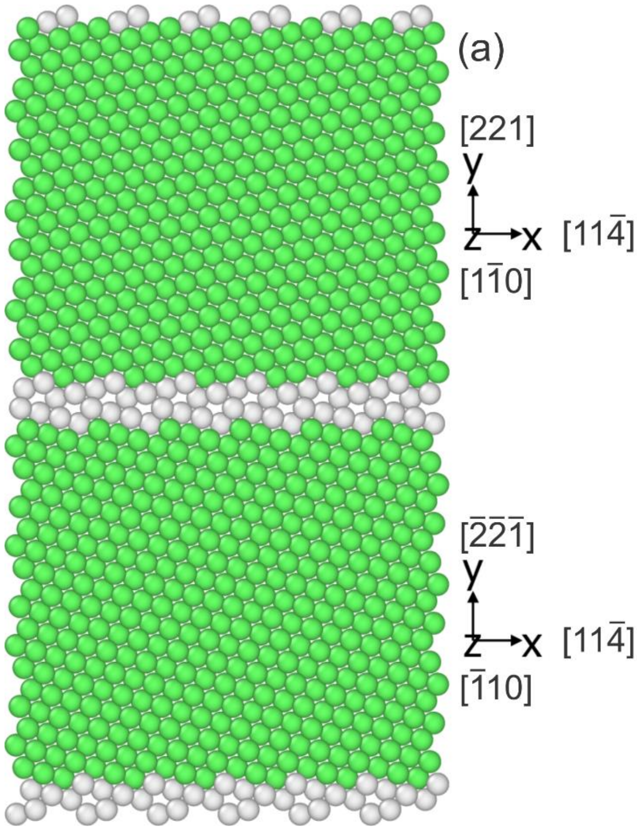

Figure 2: OVITO visualizations of the simulated bicrystal model (a) Relaxed structure of an Ag Σ9 (221) symmetric tilt GB (b) Close-up of the GB and E structural units.

The bicrystal was initially generated as pure Ag, then energy minimized using the conjugate gradient method. The resulting structure was then imported to OVITO. Using adaptive common neighbor analysis, all particles of structure type "other" were determined to be grain boundary atoms. Particles with a centrosymmetry parameter greater than 0.01 were designated as grain boundary adjacent. Then, the particle with the smallest centrosymmetry parameter was chosen as the reference bulk atom. The simulation was then run again using the algorithm described in Section 2.1 to generate $E^{gb}_{solute_i}$ for use in Equation (5). This completed the data generation for a one solute segregation energy study.

2.2.2. Polycrystal

The simulated polycrystal was a pure Ag cube of side 30 nm with six randomly oriented and randomly distributed grains created in the software Atomsk using the Voronoi tessellation scheme [23]. The model had periodic boundary conditions on all sides. The structure was then energy minimized using the conjugate gradient method, and thermally annealed using a Nose-Hoover thermostat and a Parrinello-Rahman barostat held at 500 K and zero pressure for 50 ps. Then, the structure was cooled to 1 K at zero pressure over 40 ps in accordance with the methods shown by Wagih et al. [8]. The polycrystal was then energy minimized again using conjugate gradient method with energy (eV) and force (eV/Å) tolerance stopping criteria of 10^{-8} and maximum evaluations set to 10^{3} evaluations.

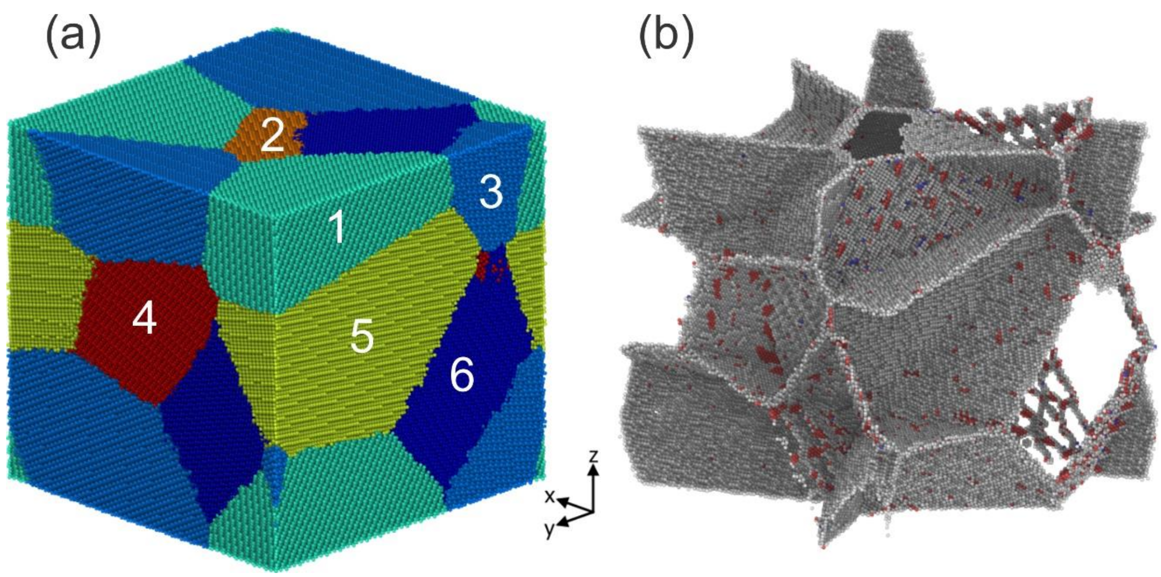

Figure 3: Simulated polycrystal model. (a) the pure Ag polycrystal grain structure. (b) the isolated GBs for the pure Ag polycrystal

The final configuration of the polycrystal a GB atom fraction of 9.1%, with a total of 1,578,562 atoms. The largest grain consisted of 19.9% of the atoms, and the smallest consisted of 12.6%. The average grain size was ~20 nm.

2.3 Data Reduction

For each GB, the list of E_{solute}^{gb} and correlating particle ID's from the LAMMPS simulation, as well as E_{solute}^{c}, were inserted in Equation (5) to find the atomic site-specific segregation energy, E_{seg_i}, for each GB site. The resulting list of atomic site-specific segregation energies was plotted as a probability mass function for further analysis. For the polycrystal model, the list of atomic site-specific segregation energies was analyzed using the Bayesian Information Criterion functionality of the mclust package in the software R to determine the probability density function that best fits the probability mass function produced by the simulation [24, 25]. Due to the random orientation of the grain boundaries in the polycrystal, we allowed for multi-modal distribution fit. The coefficient of determination, R^2, was then used to determine the quality of fit.

CHAPTER 3: Bicrystal Segregation Energy

3.1. One Solute Segregation

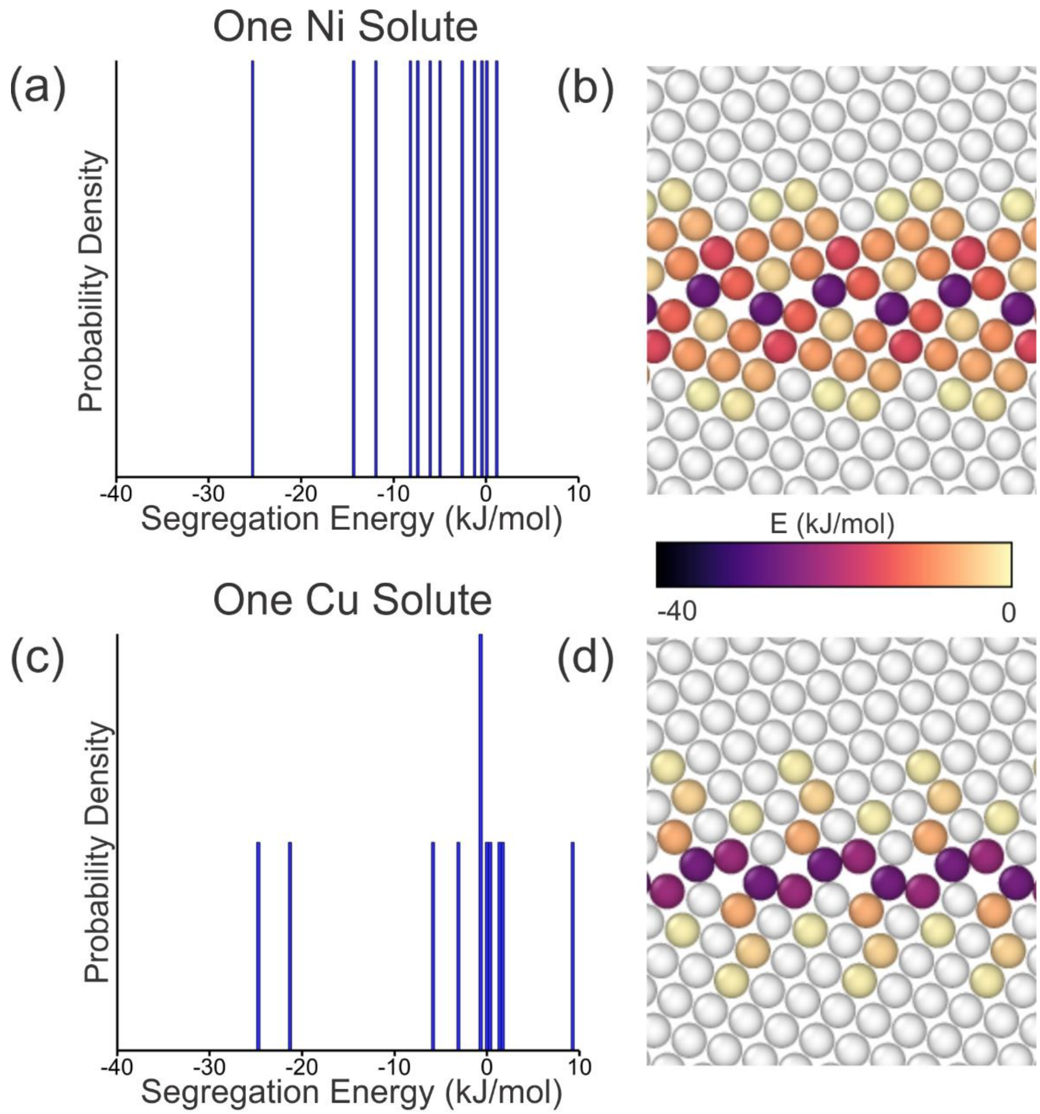

Figure 4: Atomic site segregation energies in a Σ9 (221) Ag bicrystal. (a) One Ni solute segregation energy probability distribution, (b) heat map of atomic site segregation energy of one Ni solute in the Ag bicrystal, (c) One Cu solute segregation energy probability distribution, (d) heat map of atomic site segregation energy of one Cu solute in the Ag bicrystal.

Figure 2(b) shows that the simulated Σ9 (221) Ag bicrystal model contains a GB made of a repetition of E structural units, with twelve distinct atom sites between the GB and GB adjacent test sites. Therefore, it is found in Figure 4 that there are only twelve different E_{seg} values predicted with one solute. For an Ni solute, in Figure 4(a), eight of those sites are shown to exhibit favorable GB segregation with a negative segregation energy. The average segregation energy over all sites is equal to -6.76 kJ/mol with one Ni solute. For a Cu solute, in Figure 4(c), six distinct GB atomic sites are found to be favorable GB segregation (negative E_{seg}) sites. The average segregation energy over all sites is -3.95 kJ/mol.

To better visualize the spectrum of segregation energy in the context of this GB, we produce a heatmap where each atomic site is color coded in accordance with its atomic site segregation energy. Sites with the most negative segregation energies (most favorable) are colored darkest, and sites with a segregation energy greater than or equal to zero (not favorable) are colored white for clarity. In Figure 4 (b) and (d) we see that the site most prone to GB segregation was the same for both models, with only a 0.4 kJ/mol difference between the two models. However, for the Ni solute model, the second most prone site type was farther away from the GB, while in the Cu solute model, it remained in the GB. Interestingly, while the Ni model has more segregating sites than the Cu model, the second most prone site in the Cu model has a segregation energy 7 kJ/mol less than that of the Ni model.

3.2. Two Solute Interactions

To study the local effects of solute-solute interactions at a Σ9 (221) GB, the algorithm was adapted for two solutes as follows. First, the particle site with the largest (i.e., most negative) segregation energy was chosen as a fixed solute site, since it was the most likely site for the first solute atom to be organically. Then, the bulk energy was calculated as the minimized energy of a system with two solute atoms, one at the bulk site and one at the fixed site. The solute energy was calculated as that of a system with two solute atoms, at the fixed site and at the *i*th GB site, respectively. Lastly, the same MS algorithm was run over all GB atomic sites with the slight change of keeping a solute atom in the fixed site for the entire simulation.

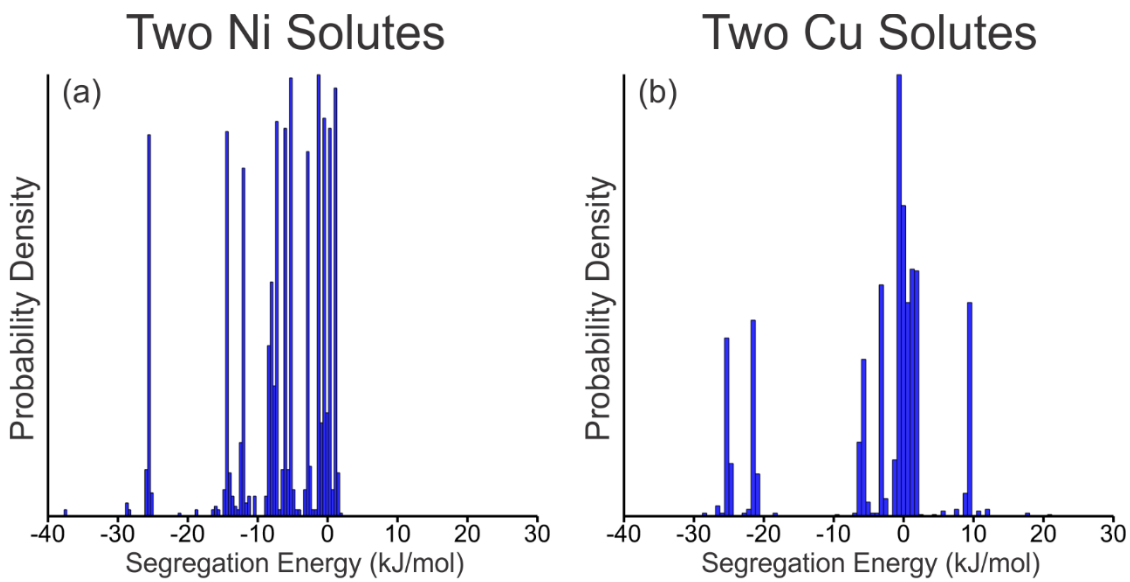

Figure 5: Segregation energy probability distribution in a Σ9 (221) symmetric tilt boundary Ag bicrystal with (a) two Ni solutes and (b) two Cu solutes.

For the Ni-Ni solute interaction, in Figure 5(a), the average segregation energy was found to be -6.89 kJ/mol, with 83% of the GB and GB adjacent sites prone to segregation. For the Cu-Cu interaction, in Figure 5(b), the average segregation energy was found to be -3.89 kJ/mol with 59% of GB and GB adjacent sites prone to segregation. The probability distribution for both models is similar to that of the one solute segregation study in Figure 4 (a) and (c) except for a spreading from the original energies of the twelve GB sites, which is attributed to the solute-solute interactions near the fixed solute. Furthermore, the Ni model’s average segregation energy decreased from the one solute model, implying that this model is more prone to segregation once there is a fixed solute in the GB. On the contrary, the Cu model's average segregation energy increased from the one solute model, implying that this model is less segregation prone. Given that both models showed an increased number of segregating sites, but opposite effects on total average segregation energy, we must consider the local environment effects on GB segregation near the fixed solute.

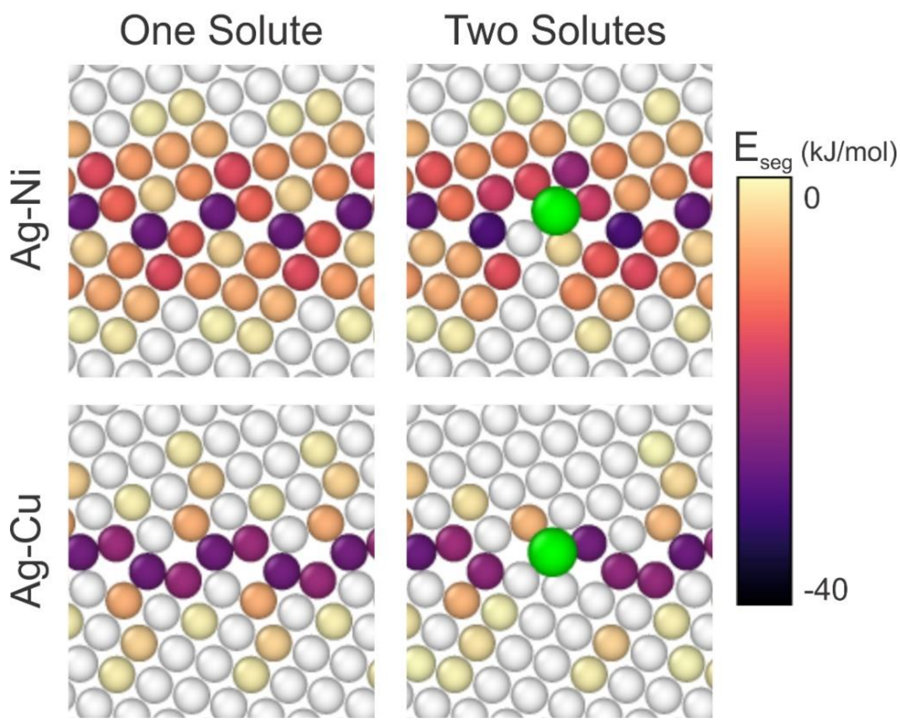

Figure 6: Heatmap of segregation energy near the fixed solute site for Ag-Ni and Ag-Cu. The fixed solute is highlighted in green color.

We studied the segregation energy at the 24 nearest neighbors to the fixed solute, hereby referred to as the local environment. Figure 6 shows a close-up of the heat map for one and two solutes for both models. For the Ni model, it appears that the segregation energy in the local environment became more negative in the two-solute study, whereas most of the nearest sites in the Cu model have positive segregation energy. However, outside of the local environment the segregation energy for both models appear to be consistent between the one and two solute studies.

3.3. Local Environment Analysis

To verify the qualitative observations from Section 3.2, we compare the average segregation energy in the local and non-local environments between one and two solutes. To quantitatively determine the effect of solute-solute interaction on segregation energy we define two zones of interest: the local environment and the non-local environment. Note here that since there is no data point in the two-solute study at the fixed solute atomic site because that site can only be occupied by one solute, the local environment does not include that atomic site. The non-local environment contains each of the test GB atomic sites not included in the local environment. We computed the average segregation energy in these two zones for the one and two solute studies. We then compared them by calculating ΔE_{seg}, the difference in average segregation energies between one and two solutes. The results are presented in Table 1.

Table 1: Average segregation energies in a Σ9 (221) Ag GB (kJ/mol).

	Ni Solute		Cu Solute	
	Local	Non-local	Local	Non-local
1 Solute (kJ/mol)	-13.03	-6.67	-10.19	-3.84
2 Solutes (kJ/mol)	-16.34	-6.76	-2.53	-3.92
ΔE_{seg} (kJ/mol)	-3.31	-0.09	7.65	-0.08

The average segregation energy within the local environment of the fixed Ni solute in the two solute study becomes significantly more negative than the average segregation energy in the one solute study. The non-local environment sees a small decrease in average segregation energy, mirroring that of the total bicrystal. This shows an attractive effect from the fixed Ni solute, which indicates that Ni-Ni solute interactions may lead to solute clustering within the GB. In the Ag-Cu study, however, ΔE_{seg} in the local environment is positive, while remaining negative in the non-local environment. This shows a repulsive effect of the fixed Cu solute within its local environment, indicating that Cu-Cu solute interactions would not lead to solute clustering within the GB.

3.4. Discussion and Conclusion

Homogeneous and heterogeneous segregation are terms typically reserved for polycrystalline structures. However, there have been previous works that show clustering within bicrystal structures may indicate a propensity for heterogeneous segregation of a bulk-solute pair in polycrystals. O’Brien et al. [16] showed multiple different ordered bicrystal GBs in which MC/MD simulations of Pt solute in Au had distinct low and high solute concentration areas within the GB. This study then moved on to show heterogeneous segregation behavior of Pt in an Au polycrystal. Pan et al. [11] also has shown MC simulations of Cu and Ni in Σ9 (221) and Σ11 (113) Ag bicrystal with clustering of Ni solute and an even distribution of Cu solute across multiple solute concentrations. In this thesis, we find that an Ni atom in a Σ9 (221) Ag bicrystal GB has an attractive effect for a second Ni atom in its local environment, which we conclude to be an indicator for solute clustering. We also find that a Cu atom in the same GB has a repulsive effect on a second Cu atom in its local environment, which implies that solute clustering would be less favorable. Given these results, it follows that the same indications from these bicrystals can be applied to polycrystalline structures. To evaluate this hypothesis, we look to our polycrystal study in Chapter 4.

CHAPTER 4: Polycrystal Segregation Energy

4.1 One Solute Segregation Spectra

Solute segregation in a polycrystal was simulated to expand the bicrystal analysis in Chapter 3 because it more accurately represents segregation behavior for practical use in material design. The probability distributions for one solute of Ni or Cu in an Ag polycrystal are presented in Figure 7.

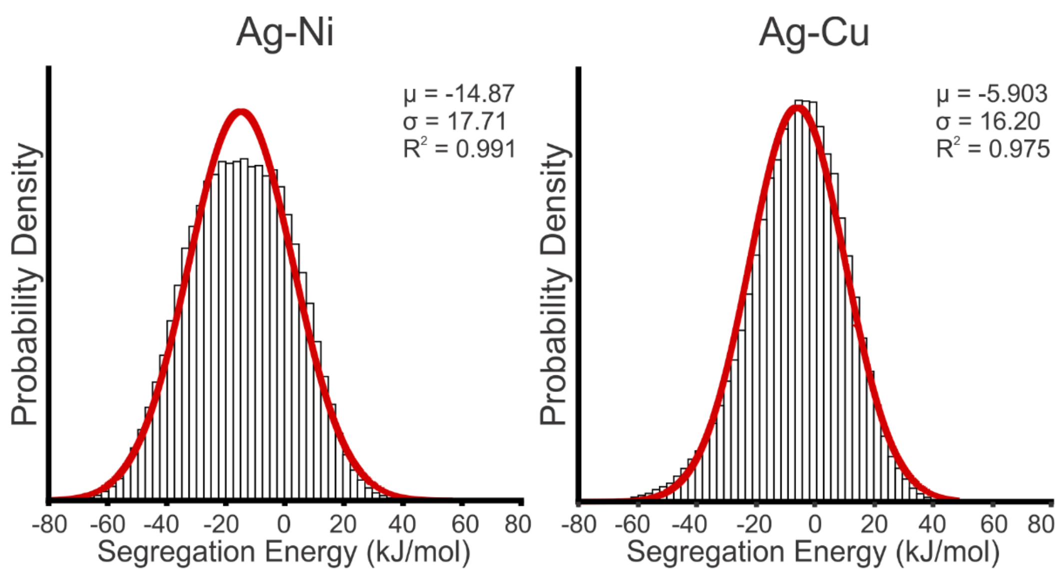

Figure 7: Probability distributions of GB segregation energy in a randomly oriented 30nm Ag polycrystal with (a) one Ni solute or (b) one Cu solute, where μ is the location parameter (kJ/mol), σ is the scale parameter, and R^2 is the coefficient of determination.

The segregation energy spectra in Figure 7 agree with previous studies [8-10], showing that site specific segregation energy spectra in randomly oriented polycrystals follow a normal distribution. Therefore, the location and scale parameters of the normal distribution, μ and σ, respectively, correspond to the average and the standard deviation of the segregation energy. We find that both Ni and Cu solutes are associated with a negative average segregation energy in Ag polycrystals, which is indicative of a favorable GB segregation. In the total polycrystal, 78% of GB atom sites are favorable for Ni solute, and 62% of sites are favorable for Cu solute. Since our algorithm was started with the same Ag polycrystal model for both Ni and Cu solutes, this result supports our hypothesis from the one-solute bicrystal study that combined structural and chemical characteristics influence the segregation behavior at each GB site where the solute is placed.

4.2 Equilibrium Solute Segregation using MC/MD Simulations

To study the effects of solute-solute interactions on segregation energy at random GBs in the polycrystal, we first determined that it would be more meaningful to isolate individual GBs within the polycrystal based on their equilibrium segregation behavior at high solute content. This conclusion is drawn from the results of the bicrystal study showing that there is a distinct local environment effect at a fixed solute within the GB. To choose which GBs to test, we executed MC/MD simulations of equilibrium segregation of Ni solute and a Cu solute within the same Ag polycrystal. Subsequently, each interface was isolated in both the Ni and Cu solute simulation models using OVITO to generate a new GB atom list, and their one-solute segregation energy was extracted from the total polycrystal data. Then, the same procedure from the two-solute bicrystal study is followed for each of the three chosen GBs. MC/MD simulations were performed to in accordance to the methodology by Pan and Sansoz [11], with a total solute concentration of 4 at.%. It has been shown by Picard [26] that this solute concentration yields to heterogeneous segregation of Ni solute in Ag polycrystals in MC/MD simulations. From our Ag – 4at.% Ni simulation, three GB configurations were identified as most representative. The first interface is highly saturated with Ni solute at a concentration of 46.9% referred to as GB

A in Figure 8. This configuration is similar to an amorphous film complexion described in the literature by Schuler and Rupert [27]. The next is a GB interface with heterogeneous clustering at an Ni solute concentration of 14.3% referred to as GB B in Figure 8. Lastly, we choose a GB triple junction with an Ni solute concentration of 28%, which is approximately equal to the total GB solute concentration for the polycrystal model, i.e. 27.6% Ni.

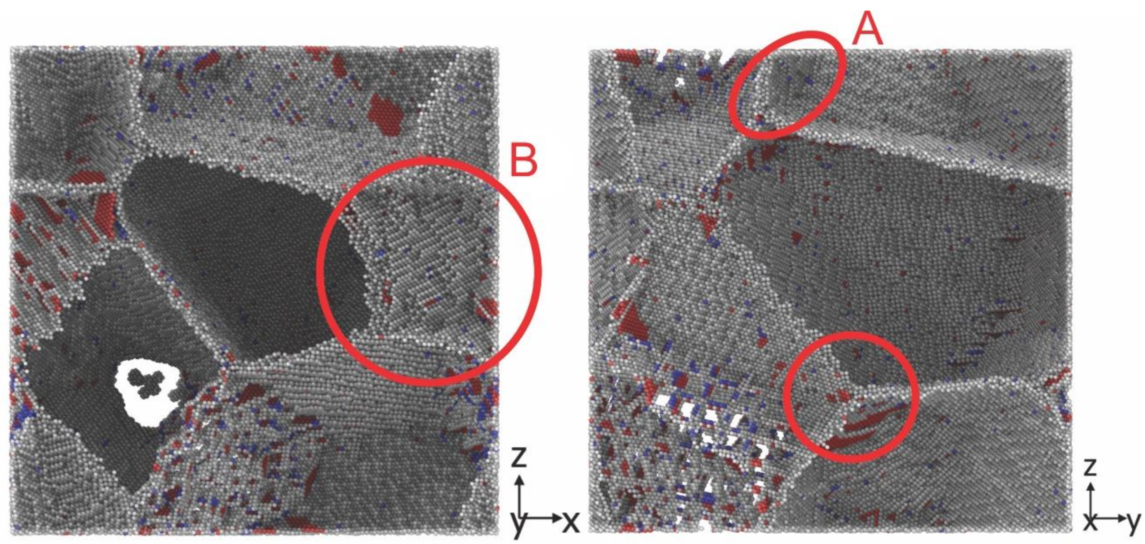

Figure 8: Locations of representative interfaces referred to as GB A, GB B, and GB triple junction in the polycrystal.

Furthermore, we simulated each of these GBs with MC/MD solute simulation of Ag – 4at.% Cu and find evenly distributed Cu solutes in each GB, with local solute concentration of 21.3%, 22.1%, and 24.1% for GB A, GB B, and the triple junction, respectively. The GB solute concentration for the total polycrystal is 22.3%, so the test GBs are accepted as having typical homogeneous segregation behavior for this model. The isolated solute atoms for each chosen GB configuration can be seen in Figure 9.

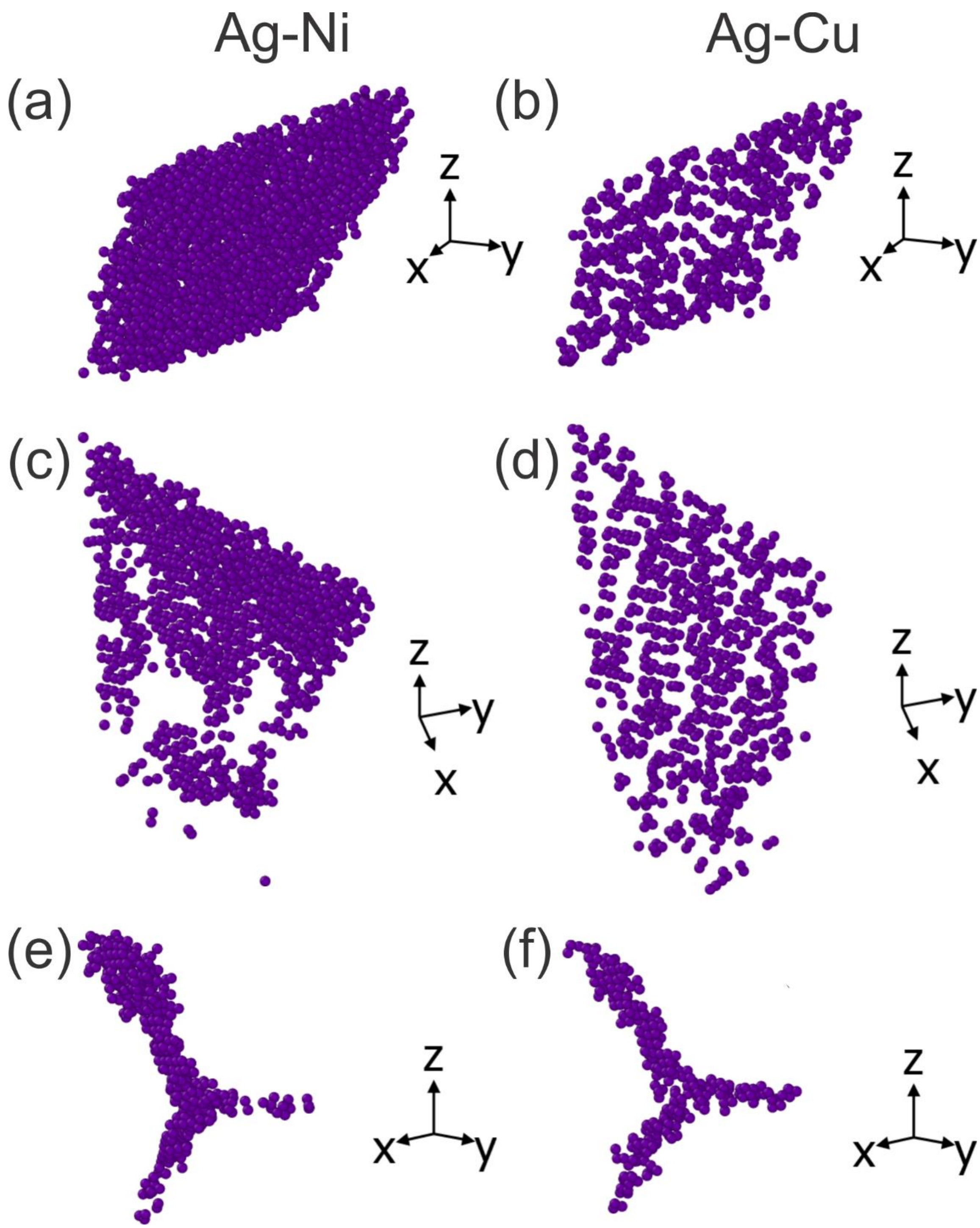

Figure 9: Close up MC/MD simulation snapshots of equilibrium solute segregation (Ni vs Cu at 4at.%) in isolated GB region of an Ag polycrystal. (a)-(b) GB A, (c)-(d) GB B, (e)-(f) GB triple junction.

4.3 Two Solute Interaction using the MS Algorithm

4.3.1. GB A

Recall that GB A was chosen as a test interface because it was a highly solute saturated GB in the Ni MC/MD study with a concentration of 46.9% Ni solute. To complete the two-solute study for GB A, first we extract the one-solute segregation energy data for this GB from that of the total polycrystal for both Ni and Cu solutes as shown in Figure 12 (a) and (b). We choose the atomic site with the most negative segregation energy as the fixed solute position. We then re-run the simulation, scanning only the atomic sites in GB A to generate the two-solute segregation energy data, seen here in Figure 12 (c) and (d).The resulting segregation energy spectra are shown below in Figure 10.

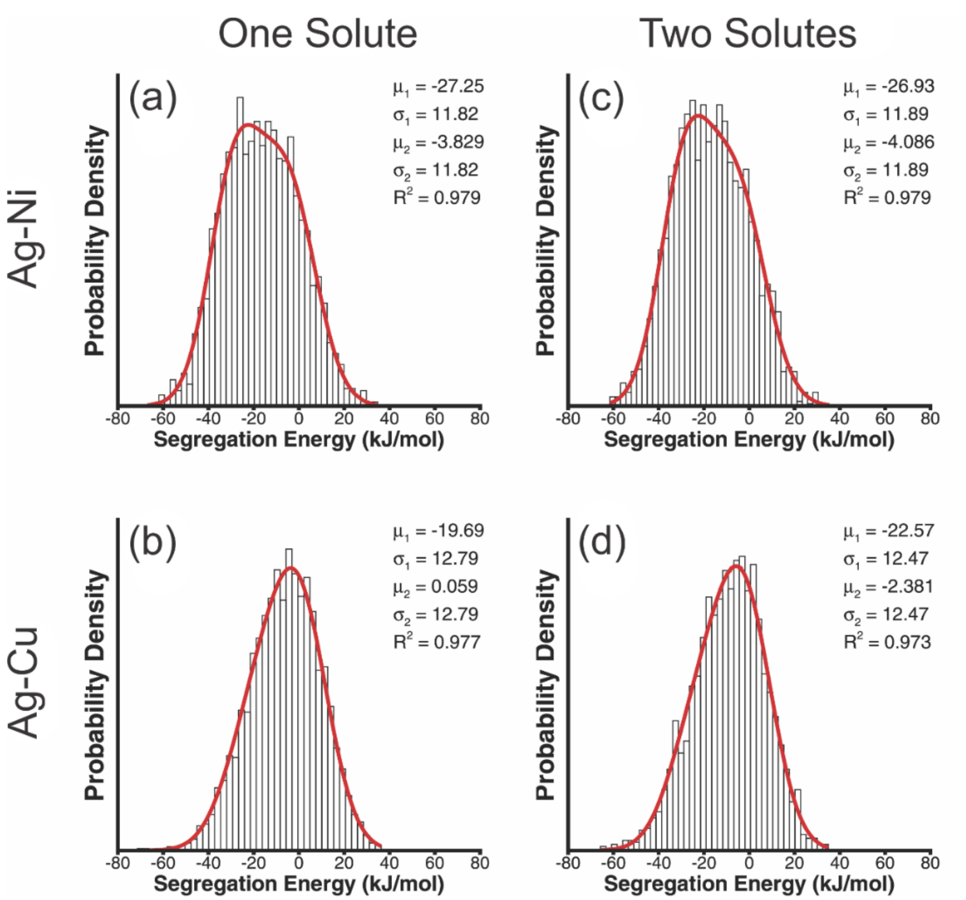

Figure 10: Probability distribution of solute segregation energy in GB A for (a) one Ni solute (b) one Cu solute (c) two Ni solutes (d) two Cu solutes.

In Figure 10, all four probability distributions are best described by five characteristic values: μ_1, μ_2, σ_1, σ_2, and R^2. In the Cu model for both one and two solutes, we see this presenting as a slightly skewed distribution. However, in the Ni model, there seems to be a slight separation of two peaks in the distribution, so we consider the possibility of a bimodal distribution. A distribution can only be considered bimodal if the two peaks, μ_1 and μ_2, are separated by more than twice the average of the two standard deviations, σ_1 and σ_2. In each case for GB A, these distributions are distinctly unimodal because they do not meet the required peak separation to be considered bimodal. Since these distributions are still best described by multiple μ and σ values, we treat changes in these values the same as we would in a true normal distribution. In Figure 10 (a) and (b), we see a slight shift in μ_1 and μ_2, bringing them closer together. In Figure 10 (c) and (d) we see that for the Ag-Cu model μ_1 and μ_2 both become more negative for the two-solute segregation energy distribution. For further investigation of solute-solute interaction effects in GB A, we directly study the local environment effects on segregation energy by examining the heat maps in Figure 11.

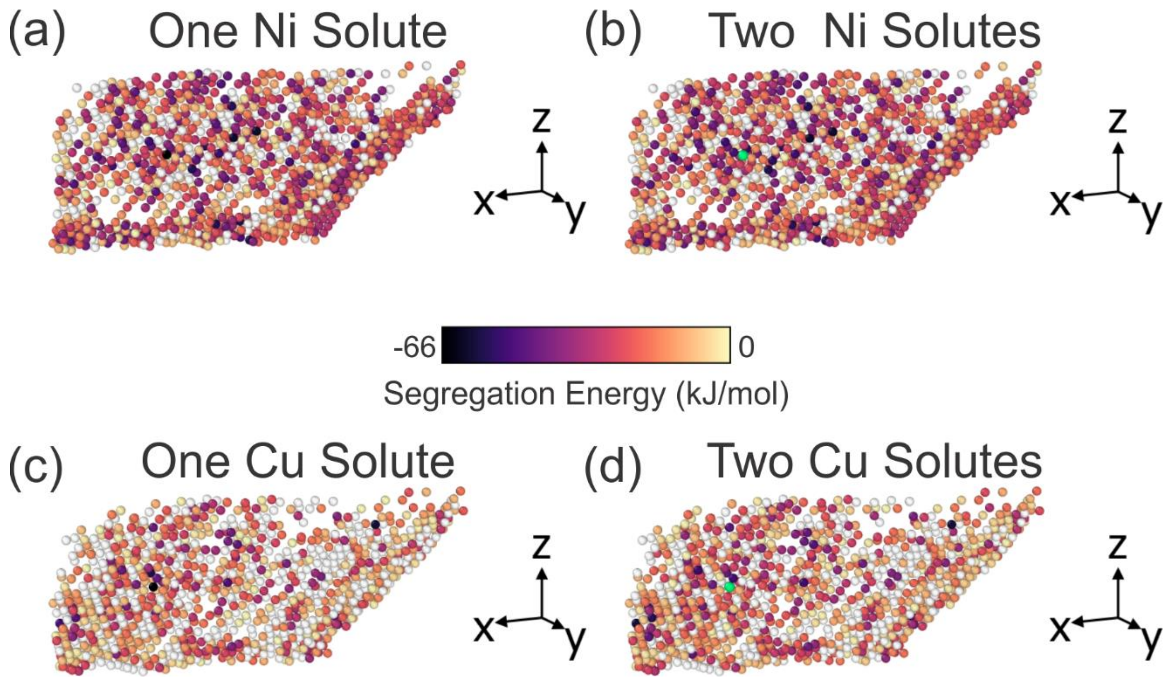

Figure 11: Heat map of the segregation energy spectra sliced to display the fixed solute atomic site in GB A for (a) One Ni solute, (b) Two Ni solutes, (c) One Cu solute, (d) Two Cu solutes. Fixed solute atom in (b) and (d) highlighted here in green.

Visual comparison of the differences between the one and two solute studies is difficult due to the random orientation of GB A. However, since the Ni and Cu models share their range of segregation energy, we can compare the differences between solute types. Qualitatively, we can see that the Ni model has more atomic sites that are prone to solute segregation than Cu. This distribution mirrors the behavior seen by the solute concentration of GB A between the two solute types for the MC/MD Ag – 4at.% solute simulations. To further validate our assertion that the presence of multiple characteristic values in a distribution of segregation energies does not inherently alter how changes in those values should be interpreted, we apply the local environment analysis methodology presented in Section 3.3. Recall that we consider the local environment to be the 24 atomic sites nearest the fixed solute atomic site, and the non-local environment to be all atomic sites in the GB not included in the local environment.

Table 2: Local environment analysis of average segregation energies (kJ/mol) in GB A.

	Ni Solute		Cu Solute	
	Local	Non-local	Local	Non-local
1 Solute (kJ/mol)	-21.55	-16.40	-18.45	-6.26
2 Solutes (kJ/mol)	-26.54	-16.82	-13.17	-8.96
ΔE_{seg} (kJ/mol)	-4.99	-0.42	5.27	-1.58

Table 2 shows that the Ni solute model has a negative change in average segregation energy in the local environment of the fixed solute, while the Cu solute model has a positive change in average segregation energy in the local environment of the fixed solute. This indicates that the fixed solute has an attractive effect in the local environment for a second Ni solute and a repulsive effect for a second Cu solute. These findings agree with those from the bicrystal study, however it remains unclear what the effect of the movements of μ_1 and μ_2 with respect to each other is, as opposed to their movement in relation to 0 kJ/mol. It is interesting to note here that the Cu solute showed more of an effect on the non-local environment than the Ni model.

4.3.2. GB B

GB B was chosen for its heterogeneous clustering segregation behavior in the Ag – 4at.% Ni MC/MD simulation, and evenly distributed segregation behavior in the Ag – 4at.% Cu MC/MD simulation, as seen in Figure 9 (c) and (d). We apply our MS algorithm using the same methodology described for GB A. The resulting energy spectra are shown in Figure 12.

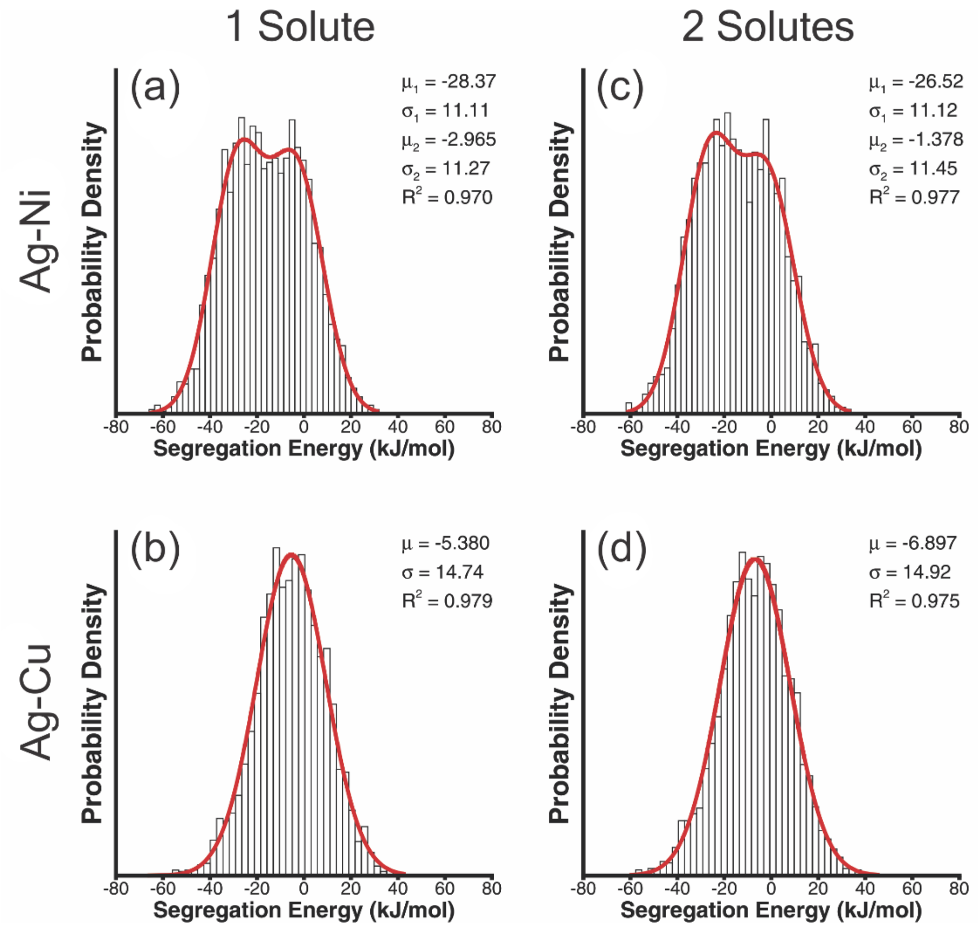

Figure 12: Probability distribution of GB segregation energy in GB B. (a) One Ni solute (b) One Cu solute (c) Two Ni solutes (d) Two Cu solutes.

In Figure 12 (a) and (c) we find a bimodal normal distribution for one and two solutes in the Ag-Ni model, and in Figure 12 (b) and (d) we find a standard normal distribution for one and two solutes in the Ag-Cu model. The bimodal peak separation condition is met by the segregation energy distribution of Ni in GB B for both the one and two solute studies, and thus we must acknowledge the novel implications of a bimodal segregation energy distribution. A bimodal normal distribution is simply the mixture of two normal distributions, and up until this point, we have considered the normal distribution of segregation energies to be representative of solute segregation behavior.

Given this, it is possible that the presence of a bimodal distribution of atomic site segregation energy may indicate two distinct segregation patterns in an individual GB, however further investigation of this line of questioning is outside the scope of this thesis. Henceforth, we consider the movement of the two peaks of any bimodal distribution in the same manner as the movement of the peak of a standard normal distribution.

In Figure 12 (a) and (c) for Ni solutes in GB B, μ_1 and μ_2 are both more positive with two solutes than in the one solute segregation study. This contradicts the initial hypothesis for Ni-Ni solute interaction based on the bicrystal study where it was found that Ni-Ni interaction promotes solute clustering within the GB. In the bicrystal study and in GB A, we determined that a negative change in total average GB segregation energy correlated to attractive solute-solute interactions. The results of the one and two solute Cu studies in Figure 12 (b) and (d) are also in disagreement with the previous results. The average segregation energy in the two solute study is more negative than that of the one solute study. However, we found in the bicrystal and in GB A that Cu-Cu interaction did not promote solute clustering within the GB. As determined by our investigation into GB A, since the meaning behind segregation energy spectra with multiple sets of characteristic values is unknown, these observations are inconclusive on their own. Figure 13 presents the heat maps of the segregation energy spectra on GB B.

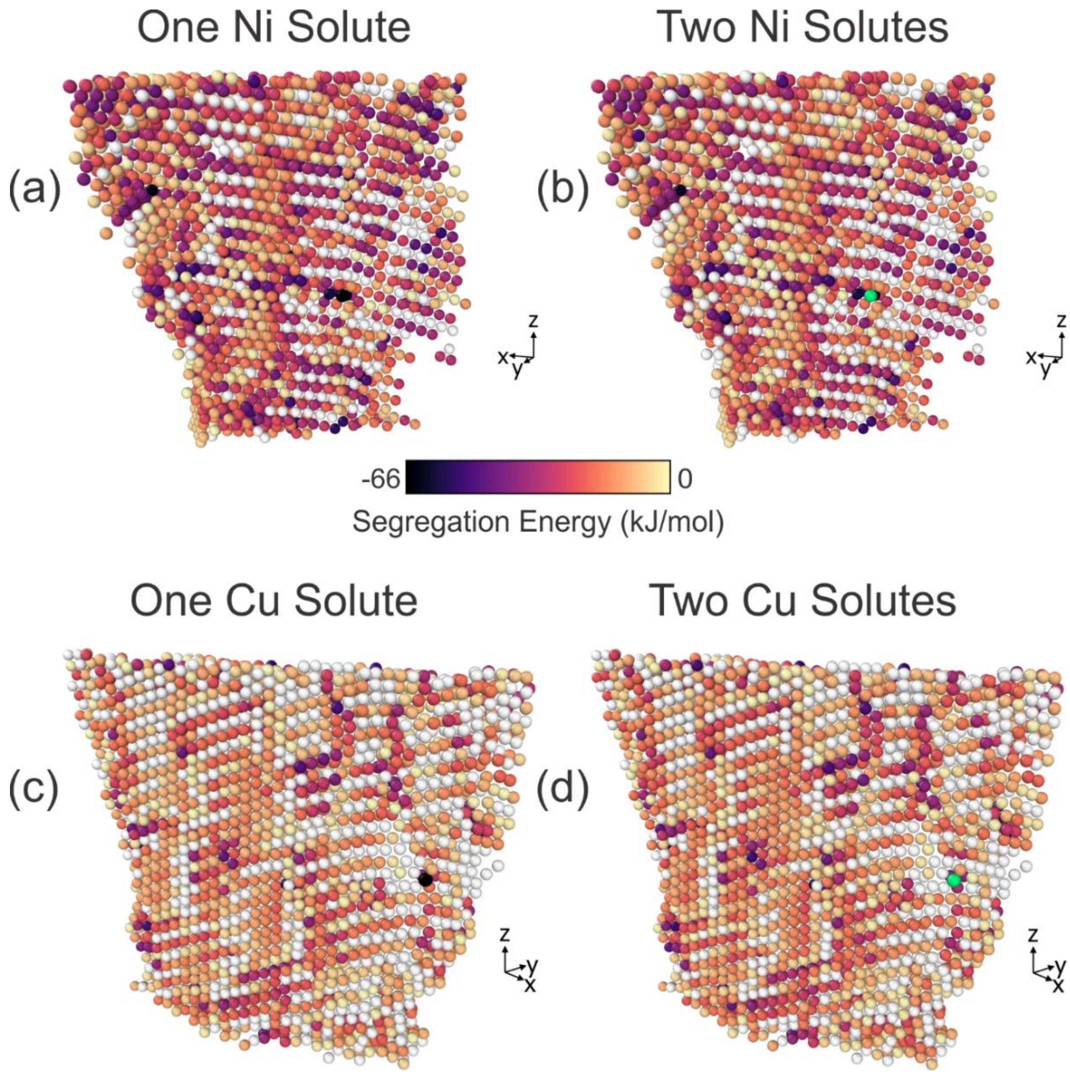

Figure 13: Heat map of the segregation energy spectra sliced to display the fixed solute atomic site in GB B for (a) One Ni solute, (b) Two Ni solutes, (c) One Cu solute, (d) Two Cu solutes. Fixed solute atom in (b) and (d) highlighted here in green.

In Figure 13, we show the same cross sections of GB B for the Ag-Ni and Ag-Cu models. Due to the random orientation of GB B, it is difficult to qualitatively assess the differences between the one and two-solute studies for both models and determine why we see the unexpected changes in average segregation energy described above. To explain this discrepancy, we consider the local environment effect on segregation near the fixed solute using the methodology described in Section 3.3.

Table 3: Local environment analysis of average segregation energies (kJ/mol) in GB B.

	Ni Solute		Cu Solute	
	Local	Non-local	Local	Non-local
1 Solute (kJ/mol)	-29.58	-15.75	-3.21	-5.36
2 Solutes (kJ/mol)	-27.90	-14.27	1.43	-6.94
ΔE_{seg} (kJ/mol	1.67	1.48	4.64	-1.58

In the results of the Cu solute in Table 3, we can see that even though the total GB segregation energy becomes more negative in the Cu model, as seen in Figure 12 and in the non-local energy, there is a repulsive effect of the fixed solute in its local environment. This conclusion agrees with the Cu results from the bicrystal and GB A in Table 1 and 2. However, in Table 3, the Ag-Ni model has the same inconsistency in the local environment analysis as was found from the segregation energy spectra in Figure 12. To further investigate this, we study the position of the fixed Ni atomic site in the MC/MD Ag – 4at.% Ni simulation, henceforth referred to as "Atomic Site 1."

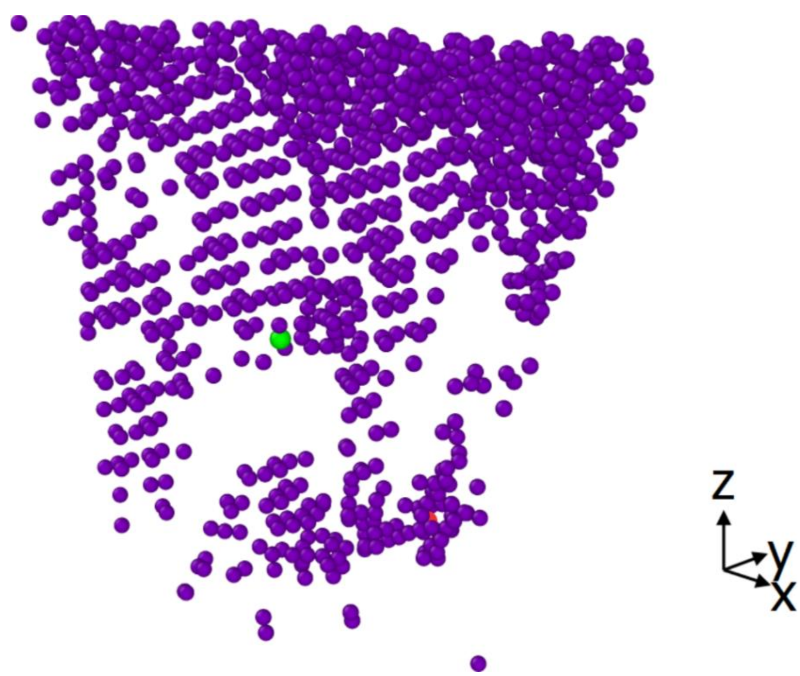

Figure 14: Position of Atomic Site 1 in GB B of the MC/MD Ag – 4at.% Ni simulation, highlighted in green, found to be on the edge of a solute void area. Position of Atomic Site 2, highlighted in red, found in a solute cluster.

As seen in Figure 14, Atomic Site 1 is filled with an Ni solute atom in the MC/MD study, implying that our methodology for choosing a fixed solute site is reasonable. However, the equilibrium position of that site is on the edge of a GB area void of Ni. Thus, the explanation of the repulsive effect found in the local environment of Atomic Site 1 may be the same reason that it is not in a cluster in the MC/MD simulation. To determine if the attractive effect we were expecting does exist in this GB, we choose a second test site, Atomic Site 2. Atomic Site 2 is chosen by finding a site in one of the clustering regions from the MC/MD study that correlates to a negative segregation energy in the one-solute Ni simulation. We then repeat the two-solute study for the Ag-Ni model, and immediately look to a local environment analysis to determine the Ni-Ni solute interaction effect.

Table 4: Local environment analysis of average segregation energies (kJ/mol) in GB B for Atomic Site 2.

	Ni Solute	
	Local	Non-local
1 Solute (kJ/mol)	-11.58	-15.89
2 Solutes (kJ/mol)	-14.50	-15.64
ΔE_{seg} (kJ/mol)	-2.92	0.25

In Table 4 we find that the difference in average segregation energy in the local environment of Atomic Site 2 is negative. This corresponds to the expected attractive effect of the fixed Ni solute within its local environment when clustering is present in the MC/MD simulation. Since we are able to distinguish an atomic site that corresponds to a solute void area from an atomic site that corresponds to a solute cluster in the MC/MD Ag – 4at.% Ni simulation, we confirm that the present MS algorithm does not blindly determine clustering or non-clustering solely based on chemical interactions of the two solutes, but also takes local GB structure effects into account.

4.3.3. Triple Junction

The third polycrystal GB interface studied in this thesis was a GB triple junction. We include this interface to determine if there are any inherent structural effects of three intersecting GBs on atomic site segregation energy. We continue the same methodology for applying our MS algorithm and present the results in Figure 15.

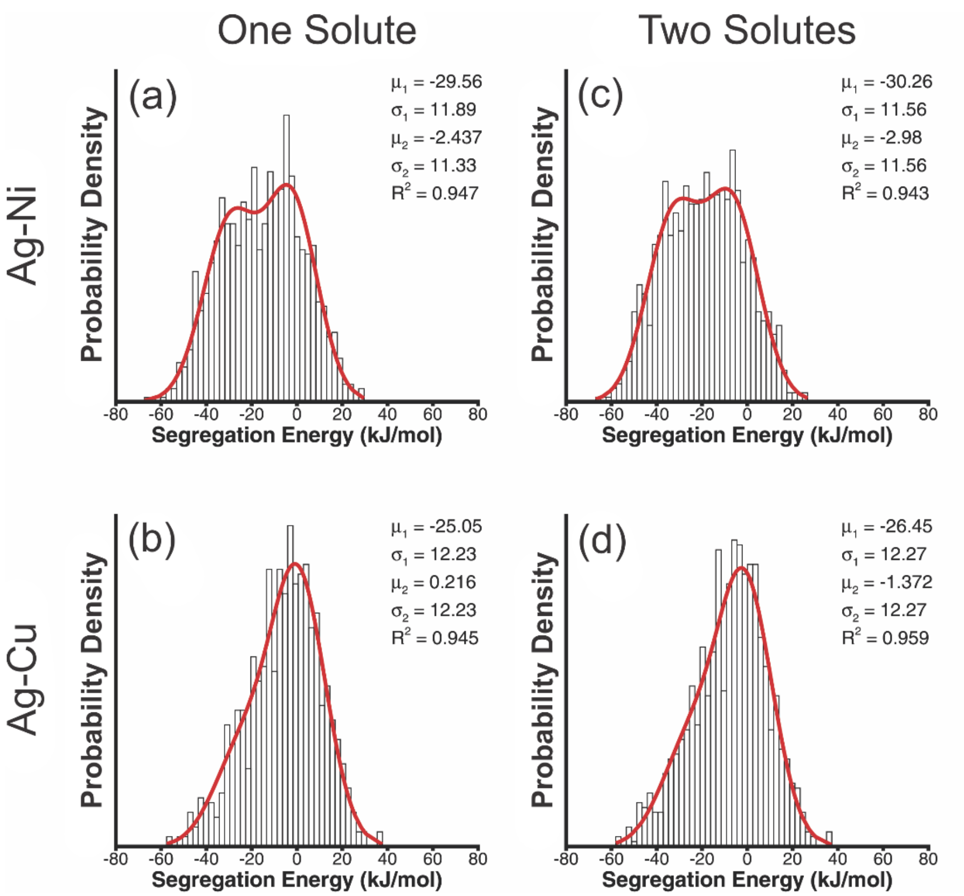

Figure 15: Probability distribution of solute segregation energy in the test triple junction for (a) one Ni solute (b) one Cu solute (c) two Ni solutes (d) two Cu solutes.

As we can see in Figure 15, again all four distributions are described by five characteristic values. The one and two-solute segregation energy distributions for the Ag-Ni both meet the conditions for bimodality, and the Ag-Cu distributions are again unimodal. Interestingly, this is the only GB interface in which both μ_1 and μ_2 become more negative in the two-solute study for both Ag-Ni and Ag-Cu. This is also the only GB in which μ_1 and μ_2 move farther apart in the two-solute study for both Ag-Ni and Ag-Cu. The Cu distributions also appear to be more skewed for this GB than the others.

Table 5: Local environment analysis of average segregation energies (kJ/mol) in the test GB triple junction.

	Ni Solute		Cu Solute	
	Local	Non-local	Local	Non-local
1 Solute (kJ/mol)	-18.41	-14.54	-16.45	-5.81
2 Solutes (kJ/mol	-19.78	-13.85	-14.59	-7.77
ΔE_{seg} (kJ/mol)	-1.37	0.69	1.85	-1.95

In Table 5 the local area analysis shows an attractive tendency for the Ni model and a repulsive tendency for the Cu model as seen in atomistic site 2 in GB A, GB B, and the bicrystal. However, this GB exhibits the least effect within the local environment out of the three GB types studied for both Ni and Cu solutes. This GB is also the only GB that sees a positive change in average segregation energy in the non-local environment with a negative change in average segregation energy for Ni solute. While the opposite effect is seen in every test GB for Cu solute, until this point, the change in average segregation energy in the local and non-local environment for Ni has been either both positive or both negative.

4.4 Polycrystal Discussion and Conclusion

In this chapter, we use the methodology developed in the bicrystal study to predict solute-solute interactions in representative polycrystal GB interfaces. We find that our predictions of the local environment effect of fixed Ni and Cu solutes are accurate to the segregation behavior displayed in the MC/MD Ag – 4at.% solute simulations used to choose the test interfaces for both clustering and non-clustering behavior. Specifically, we find that this methodology not only accurately predicts Cu solute aversion to clustering in each GB interface, but also the Ni clustering in areas of GBs where the MC/MD simulation is solute saturated and aversion to clustering where it is solute void.

In this chapter, we also find that two of the chosen polycrystal GB interfaces have atomic site segregation energy spectra, best described by bimodal distributions. To our knowledge, this finding is novel, and further investigation is outside of the scope of this thesis. However, it should be noted that the two GB interfaces in question were GB B and the triple junction. These interfaces had a bimodal distribution for the Ag-Ni model and a unimodal distribution for the Ag-Cu model. GB B was chosen for its heterogeneous solute clustering in the MC/MD Ag – 4at.% Ni simulation, and the triple junction appears to be heterogeneously distributed in the MC/MD Ag – 4at.% Ni simulation as well. In Figure 9 (e), we find more Ni clustering in one leg of the triple junction, while the other two legs are more sparse near the edges of the test section. These interfaces in the MC/MD Ag – 4at.% Cu simulation have been determined to be representative of the total polycrystal, and thus homogeneously segregated. Therefore, there may be a correlation between bimodal segregation energy spectra and heterogeneous solute clustering within individual grain boundaries, and this should be explored further in other works.

CHAPTER 5: Conclusions and Future Research

In this thesis, we developed an MS algorithm for determining the effect of solute-solute interactions on the spectra of GB segregation energy in FCC Ag bicrystal and polycrystal structures containing Ni and Cu solutes. Local environments around segregation GB sites were analyzed to study the effect of solute-solute interactions leading to clustering. In the Ni solute models, this method accurately predicted both areas within GBs where solute clustering does and does not occur by determining whether a fixed solute has an attractive or repulsive effect on solute atoms in the surrounding atom sites. This method also accurately predicted an aversion to clustering in the Cu models. We verify the MS results in the polycrystalline model with MC/MD simulation of equilibrium atom segregation on the same Ag polycrystal with 4% solute concentration of both Ni and Cu solutes. We assert that propensity to clustering within GBs is correlated to heterogeneous GB segregation, and thus this method can be used to accelerate the study of complex GB segregation behavior.

Further research with this methodology is required before it can be effectively used to determine heterogeneous or homogeneous segregation behavior. Specifically, this methodology should be applied to an Ni void GB to determine if this methodology would predict clustering or non-clustering behavior in that region. While we have already found non-clustering behavior in a solute void area of GB B, this result should be further verified. The algorithm can also be further developed to find the average local environment effect of a fixed solute for every GB atomic site in a test material to see if specific clustering behavior can be predicted using this methodology. It is unclear if this would be more efficient than the current MC/MD methodology, however it could prove to reduce the time and computational requirements of this type of analysis. This application of the algorithm should also be applied to the alloys studied by Picard [26] to determine if it can evoke the full range of segregation behavior found in her work.

References

[1] H. Gleiter, Nanocrystalline materials, Progress in Materials Science 33(4) (1989) 223-315.
[2] K.S. Kumar, H. Van Swygenhoven, S. Suresh, Mechanical behavior of nanocrystalline metals and alloys11The Golden Jubilee Issue—Selected topics in Materials Science and Engineering: Past, Present and Future, edited by S. Suresh, Acta Materialia 51(19) (2003) 5743-5774.
[3] A.M.H.B.L.B. Nathan Heckman; Christopher Michael Barr; Timothy Allen Furnish; Khalid Mikhiel Hattar; Stephen M. Foiles; Fadi F Abdeljawad; Christoph Eberl, Fatigue Strength Scaling at the Nanoscale - Nanocrystalline and Nanotwinned Metals., TMS 2018, Phoenix, AZ, 2018.
[4] A.R. Kalidindi, T. Chookajorn, C.A. Schuh, Nanocrystalline Materials at Equilibrium: A Thermodynamic Review, JOM 67(12) (2015) 2834-2843.
[5] Z.B. Jiao, C.A. Schuh, Nanocrystalline Ag-W alloys lose stability upon solute desegregation from grain boundaries, Acta Materialia 161 (2018) 194-206.
[6] T. Chookajorn, H. Murdoch, C.A. Schuh, Design of Stable Nanocrystalline Alloys, Science 337(6097) (2012) 951-954.
[7] D. McLean, Grain Boundaries in Metals, in: Oxford (Ed.) Clarendon Press, 1957.
[8] M. Wagih, P.M. Larsen, C.A. Schuh, Learning grain boundary segregation energy spectra in polycrystals, Nature Communications 11(1) (2020) 6376.
[9] M. Wagih, C.A. Schuh, Spectrum of grain boundary segregation energies in a polycrystal, Acta Materialia 181 (2019) 228-237.
[10] M. Wagih, C.A. Schuh, Grain boundary segregation beyond the dilute limit: Separating the two contributions of site spectrality and solute interactions, Acta Materialia 199 (2020) 63-72.
[11] Z. Pan, V. Borovikov, M.I. Mendelev, F. Sansoz, Development of a semi-empirical potential for simulation of Ni solute segregation into grain boundaries in Ag, Modelling and Simulation in Materials Science and Engineering 26(7) (2018) 075004.
[12] A. Gupta, X. Zhou, G.B. Thompson, G.J. Tucker, Role of grain boundary character and its evolution on interfacial solute segregation behavior in nanocrystalline Ni-P, Acta Materialia 190 (2020) 113-123.
[13] S.M. Foiles, F.F. Abdeljawad, N. Heckman, C.M. Barr, K.M. Hattar, B.L. Boyce, D.W. Jacobson, G.B. Thompson, Heterogeneous Grain Boundary Segregation in Platinum-Gold Alloys, Sandia National Lab.(SNL-NM), Albuquerque, NM (United States), 2018.
[14] P. Lu, F. Abdeljawad, M. Rodriguez, M. Chandross, D. Adams, B. Boyce, B. Clark, N.J.M. Argibay, On the thermal stability and grain boundary segregation in nanocrystalline PtAu alloys, 6 (2019) 100298.
[15] Z. Pan, F. Sansoz, Heterogeneous solute segregation suppresses strain localization in nanocrystalline Ag-Ni alloys, Acta Materialia 200 (2020) 91-100.
[16] C.J. O'Brien, C.M. Barr, P.M. Price, K. Hattar, S.M. Foiles, Grain boundary phase transformations in PtAu and relevance to thermal stabilization of bulk nanocrystalline metals, Journal of Materials Science 53(4) (2018) 2911-2927.

[17] S. Plimpton, Fast Parallel Algorithms for Short-Range Molecular Dynamics, Journal of Computational Physics 117(1) (1995) 1-19.
[18] H.H. Wu, D.R. Trinkle, Cu/Ag EAM potential optimized for heteroepitaxial diffusion from ab initio data, Computational Materials Science 47(2) (2009) 577-583.
[19] X. Ke, F. Sansoz, Segregation-affected yielding and stability in nanotwinned silver by microalloying, Physical Review Materials 1(6) (2017) 063604.
[20] X. Ke, J. Ye, Z. Pan, J. Geng, M.F. Besser, D. Qu, A. Caro, J. Marian, R.T. Ott, Y.M. Wang, F. Sansoz, Ideal maximum strengths and defect-induced softening in nanocrystalline-nanotwinned metals, Nature Materials 18(11) (2019) 1207-1214.
[21] A. Stukowski, Visualization and analysis of atomistic simulation data with OVITO–the Open Visualization Tool, Modelling and Simulation in Materials Science and Engineering 18(1) (2009) 015012.
[22] F. Sansoz, J.F. Molinari, Incidence of atom shuffling on the shear and decohesion behavior of a symmetric tilt grain boundary in copper, Scripta Materialia 50(10) (2004) 1283-1288.
[23] P. Hirel, Atomsk: A tool for manipulating and converting atomic data files, Computer Physics Communications 197 (2015).
[24] L. Scrucca, M. Fop, T.B. Murphy, A.E. Raftery, mclust 5: clustering, classification, and density estimation using Gaussian finite mixture models, The R Journal 8(1) (2016) 289-317.
[25] R.C. Team, R: A language and environment for statistical computing, 2017.
[26] E.-A. Picard, Atomistic Simulation Study of Nickel Solute Segregation And Mechanical Behavior in Nanocrystalline FCC, BCC, and HCP Binary Alloys, Mechanical Engineering, University of Vermont, Graudate College Dissertations and Theses, 2021, p. 76.
[27] J.D. Schuler, T.J. Rupert, Materials selection rules for amorphous complexion formation in binary metallic alloys, Acta Materialia 140 (2017) 196-205.

Appendix

A. One Solute LAMMPS MS Algorithm on a Bicrystal

```
# General settings

units           metal
boundary        p p p

atom_style      atomic
lattice         fcc 4.1608
region          box block 0   12.7279220614 0 24.0000000000000000 0
8.48528137424

create_box      2 box


#pair interaction
pair_style      eam/fs/gpu
pair_coeff      * * v5_17_Ag_1Ni.eam_.fs Ag Ni

thermo          100

variable        a file gbs9 # List of GB atom particle identifiers

#variable       bulk equal 6147 # Bulk atom location

# Grain 1 region
region          upper block INF INF   12.0000000000000000 INF INF INF

# Grain 2 region
region          lower block INF INF INF   12.0000000000000000 INF INF

label           loop     #iteration restart marker

# Create grain 1
lattice         fcc 4.1608 origin   0.1178511301977579
0.1666666666666667   0.3535533905932738 orient x 1 1 -4 orient y 2 2 1
orient z 1 -1 0
create_atoms    1 region upper


# Create grain 2
lattice         fcc 4.1608 origin   0.1178511301977579
0.1666666666666667   0.3535533905932738 orient x 1 1 -4 orient y -2 -2
-1 orient z -1 1 0
create_atoms    1 region lower
```

```
set             atom $a type 2
#set            atom ${bulk} type 2

group           upper region upper
displace_atoms  all move   0.1178511301977579   0.1666666666666667
0.3535533905932738 units box
displace_atoms  upper move 2.0 0 1.0 units box
displace_atoms  all move 0.0 0 -0.5 units box

#dump           1 all custom 2000 insert_atom_$a.*.dmp id xs ys zs

# Compute energy
variable        e equal c_thermo_pe

min_style       cg
minimize        1.0e-8 1.0e-8 1000000 10000000000

print           "$a $e" append GBS9_1sol_energy.dat
#undump         1

# Reset atoms

delete_atoms    group all

# Iterate to next GB atom
next a


jump input_GBS9_spectrum loop
```

B. Two Solute LAMMPS MS Algorithm on a Polycrystal

```
# General settings
units           metal
boundary        p p p # Periodic boundary conditions

atom_style      atomic
neighbor        1.5 bin

region          box block 0 300 0 300 0 300 # Simulation box size
create_box      2 box

label           loop # Iteration restart marker

read_data       input_AgNi add append # Polycrystal input file

# Pair settings
pair_style      eam/fs/gpu
pair_coeff      * * v5_17_Ag_1Ni.eam_.fs Ag Ni


thermo          100

variable        a file GB_B # List of GB atom particle identifiers

#set            atom 130899 type 2 # bulk atomic site
set             atom 1388987 type 2# GB B atomic site 1
if              "$a == 1388987" then "next a"
set             atom $a type 2

# Compute energy
variable        e equal c_thermo_pe

min_style       cg
minimize        1.0e-8 1.0e-8 1000000 10000000000

print           "$a $e" append AgNi_GB_B_2sol.dat

delete_atoms    group all

# Iterate to next GB atom
next            a


jump            input_AgNi_Polycrystal loop
```

C. R code for Bimodal Probability Distribution Fit

```
#  Import data file and generate histogram.
E <- scan("AgNi_GBA_1sol.DAT",skip=1)

hist(E)

#  Attach mclust library.
library(mclust)

#  Fit bimodal mixture model.

EBIC = mclustBIC(E, modelNames="V")
EModel = mclustModel(E, EBIC)

#  Print model parameters.

EModel$parameters
```

D. LAMMPS Polycrystal Equilibration

```
#########################
# Title: input.EquilConfig
# Author: Zhiliang Pan
# Date: 2019-2020
#########################

# General settings
units metal
boundary p p p
atom_style atomic

read_restart restart.AgNi.StartConfig

# Set up interaction
pair_style eam/fs
pair_coeff * * v5_17_Ag_1Ni.eam_.fs Ag Ni

# Set temperature
velocity all create 500 567890
velocity all zero linear
dump 1 all custom 10000 equi.*.dmp id type x y z
thermo 100
thermo_style custom step temp pe etotal press pxx pyy pzz pxy pxz pyz
vol

timestep 0.005

reset_timestep 0
fix 1 all npt temp 500 500 0.1 aniso 0.0 0.0 0.1
run 50000
unfix 1

write_restart restart.AgNi.EquilConfig.500K

fix 1 all npt temp 500 1.0 0.1 aniso 0.0 0.0 0.1
run 40000
unfix 1

undump 1

write_restart restart.AgNi.CoolConfig.1K
write_data    data.AgNi.CoolConfig.1K
```

E. LAMMPS MC/MD 4 at.% Solute Equilibration

```
#########################
# Title: input.MCMD_500K_0.04
# Author: Zhiliang Pan
# Date: 2019-2020
#########################
#
# General variables
variable restart equal 0 ## 0: new run, 1: restart
variable mu0 equal 1.015 ## Initial chemical potential difference
delta mu0
variable murate equal -10 ## Rate of change with respect to achieved
composition,this can be estimated based on trial simulations
variable minrate equal -10 ## Minimum rate of change
variable maxdmu equal 0.1 ## Maximum change of mu allowed in each
iteration
variable temperature equal 500 ## Simulation temperature K
variable nsteps_run equal 1000 ## Number of MD steps per iteration
variable NS equal 599 ## Number of iterations
variable c0 equal 0.040 ## Target concentration c0
variable nsteps_mc equal 100 ## MD steps per MC round
variable swap_fraction equal 1.0 ## Fraction of a full MC cycle carried
out at each round
variable kappa equal 2000 ## 2000 for Ni
variable dc0 equal 0.001*${c0} ## relative toleration for composition
variable maxdc equal ${maxdmu}/abs(${murate})

# General settings
units metal
atom_style atomic

# Set up structure
boundary p p p
read_restart restart.AgNi.EquilConfig.500K
timestep 0.001
thermo ${nsteps_mc}

# Set up interaction
pair_style eam/fs
pair_coeff * * v5_17_Ag_1Ni.eam_.fs Ag Ni

# MC/MD simulation
if "${restart}==0" then "reset_timestep 0"

variable mu equal ${mu0}
fix integrate all npt temp ${temperature} ${temperature} 0.1 aniso
0.0 0.0 0.1
fix mc all sgcmc ${nsteps_mc} ${swap_fraction} ${temperature} ${mu} &
```

```
randseed 324234 &
variance ${kappa} ${c0}

#Set up output
thermo_style custom step temp atoms pe press lx ly lz f_mc[1] f_mc[2]
f_mc[3] f_mc[4]
thermo_modify flush yes
fix 4 all print ${nsteps_run} "$(step) ${mu} $(f_mc[4]) ${murate}"
file mu_c screen no
fix 5 all print ${nsteps_mc} "$(pe)" file PotEnergy screen no

dump 1 all custom 100000 mc.*.dmp id type x y z

restart 100000 restart.*.04
run ${nsteps_run}

# Simulation with auto adjusing initial chemical potential difference

label dope
variable idx loop ${NS}
variable dc equal $(f_mc[4])-${c0}
if "${dc}>${maxdc}" then "variable dc equal ${maxdc}"
if "${dc}<-${maxdc}" then "variable dc equal -${maxdc}"
variable mu1 equal ${mu}
variable c1 equal $(f_mc[4])
variable mu equal ${mu1}-${dc}*${murate}
unfix mc

fix mc all sgcmc ${nsteps_mc} ${swap_fraction} ${temperature} ${mu} &
randseed 324234 &
variance ${kappa} ${c0}
run ${nsteps_run}

variable mu2 equal ${mu}
variable c2 equal $(f_mc[4])
variable dmu equal ${mu2}-${mu1}
variable dc equal ${c2}-${c1}
variable murate1 equal ${murate}

if "(${dmu}>1e-6||${dmu}<-1e-6)&&(${dc}>${dc0}||${dc}<-${dc0})" then
"variable murate equal ${dmu}/${dc}"

if   "${murate1}<=0&&${murate}>=0"   then   "variable   murate   equal
${murate1}"

if   "${murate1}>=0&&${murate}<=0"   then   "variable   murate   equal
${murate1}"

if "${minrate}<0&&${murate}>${minrate}" then "variable murate equal
${minrate}"
```

```
if "${minrate}>0&&${murate}<${minrate}" then "variable murate equal
${minrate}"

next idx
jump input.MCMD_500K_0.04 dope

undump  1
write_restart restart.AgNi.04
```